AD-A276 982

EDGEWOOD RESEARCH, DEVELOPMENT & ENGINEERING CENTER

ERDEC-TR-111

[redacted]

REMOTE INFRARED VAPOR DETECTION OF VOLATILE ORGANIC COMPOUNDS

[redacted]

[redacted]

R.T. Kroutil
R.J. Combs
R.B. Knapp

RESEARCH AND TECHNOLOGY DIRECTORATE

G.W. Small

OHIO UNIVERSITY
Athens, OH 45701-2979

94-08068

September 1993

Approved for public release; distribution is unlimited.

U.S. ARMY
CHEMICAL
AND BIOLOGICAL
DEFENSE AGENCY

Aberdeen Proving Ground, Maryland 21010-5423

Disclaimer

The findings in this report are not to be construed as an official Department of the Army position unless so designated by other authorizing documents.

REPORT DOCUMENTATION PAGE

Form Approved
OMB No 0704-0188

1. AGENCY USE ONLY *(Leave blank)*	2. REPORT DATE	3. REPORT TYPE AND DATES COVERED
	1993 September	Final, 91 Oct - 93 Sep

4. TITLE AND SUBTITLE

Remote Infrared Vapor Detection of Volatile Organic Compounds

5. FUNDING NUMBERS

TA-DARPA 8304

6. AUTHOR(S)

Kroutil, R.T.; Combs, R.J.; Knapp, R.B. (ERDEC); and Small, G.W. (Ohio University)

7. PERFORMING ORGANIZATION NAME(S) AND ADDRESS(ES)

DIR, ERDEC,* ATTN: SCBRD-RTM, APG, MD 21010-5423

Ohio University, Department of Chemistry, Athens, OH 45701-2979

8. PERFORMING ORGANIZATION REPORT NUMBER

ERDEC-TR-111

9. SPONSORING/MONITORING AGENCY NAME(S) AND ADDRESS(ES)

Advanced Research Projects Agency
3701 North Fairfax Drive
Arlington, VA 22203-1714

10. SPONSORING/MONITORING AGENCY REPORT NUMBER

11. SUPPLEMENTARY NOTES

*When this study was conducted, ERDEC was known as the U.S. Army Chemical Research, Development and Engineering Center, and the ERDEC authors were assigned to the Research and Detection Directorates, respectively.

12a. DISTRIBUTION/AVAILABILITY STATEMENT

Approved for public release; distribution is unlimited.

12b. DISTRIBUTION CODE

13. ABSTRACT *(Maximum 200 words)*

In many open-air monitoring applications of Fourier transform spectrometry (FTS), the lack of a valid background reference spectrum limits the ability to perform quantitative measurements. Suppression of the broad band detector envelope overcomes this limitation. Interferogram processing provides a means of suppressing the broad band background, while maintaining the target spectral signatures of interest. A combination of interferogram segment selection, digital filtering, and pattern discrimination techniques achieve the background suppression of the variable broad band detector envelope. The spectral band position, width, and strength of the target vapor determine the parameters that are used for background suppression. Interferogram segment selection depends primarily on spectral band width. Digital filter design requires inputs of spectral band position and width. The pattern discrimination techniques compensate for variation in the spectral band contour with signal strength. The FTS in the laboratory and open-air trials demonstrate the utility of the background suppression approach in environmental monitoring of volatile organic compounds.

14. SUBJECT TERMS

Fourier transform spectrometry
Digital filtering
Multilinear discriminants

15. NUMBER OF PAGES

39

16. PRICE CODE

17. SECURITY CLASSIFICATION OF REPORT	18. SECURITY CLASSIFICATION OF THIS PAGE	19. SECURITY CLASSIFICATION OF ABSTRACT	20. LIMITATION OF ABSTRACT
UNCLASSIFIED	UNCLASSIFIED	UNCLASSIFIED	UL

Blank

PREFACE

The work described in this report was authorized under DARPA Task No. 8304. This work was started in October 1991 and completed in September 1993.

The use of trade names or manufacturers' names in this report does not constitute an official endorsement of any commercial products. This report may not be cited for purposes of advertisement.

This report has been approved for release to the public. Registered users should request additional copies from the Defense Technical Information Center; unregistered users should direct such requests to the National Technical Information Service.

Acknowledgments

The authors wish to thank William Fateley, Charles Chaffin, and Tim Marshall, Kansas State University, for their assistance in the collection of some active bistatic and passive training set data.

Blank

CONTENTS

LIST OF FIGURES AND TABLES

Figures

Tables

REMOTE INFRARED VAPOR DETECTION OF VOLATILE ORGANIC COMPOUNDS

1. INTRODUCTION

Environmental monitoring with Fourier transform infrared (FT-IR) spectrometry offers a robust method for the identification and quantification of various gas pollutants. Volatile organic compounds (VOCs) represent a major pollutant from industrial[1], automotive[2], and waste sight[3] sources. These VOC sources have been characterized by open path air monitoring with a variety of FT-IR spectrometer configurations. Two spectrometer configurations are active bistatic and passive (see Figure 1).[4,5,6]

The active bistatic configuration uses an infrared (IR) source and provides transmission through the target vapor to the FT-IR spectrometer. This configuration resembles the conventional laboratory spectrometer with two possible exceptions. First, the sample cell is replaced with an open path approximately 100 meters in length. Unlike the controlled laboratory cell, the gas sample parameters are determined by meteorological conditions.[7] Second, the sample is located between the IR source and interferometer, rather than between interferometer and detector. Thus, operation of the FT-IR spectrometer in the passive configuration only requires substitution of a terrestrial scene for the IR source.

The passive FT-IR spectrometer configuration relies on a radiance difference between the target vapor cloud and background for an emission spectrum. The radiance is the spectral radiant emittance scaled by an emissivity factor.[8] The spectral emittance is calculated from Plank's function and depends on temperature. Thus, the radiance difference can be interpreted primarily as a temperature difference between target vapor cloud and background.[6] Possible background scenes are terrestrial, sky, or some mixture of both terrestrial and sky. These background scenes exhibit large temporal and spatial variations. The variations are caused by the spectral dependence of emissivity values and temperature fluctuations in the atmosphere. The background variations preclude the collection of a stable background reference spectrum.

This investigation considers signal processing approaches, which do not rely on the existence of a stable reference background.[9,10] The approach suppresses the broad band detector envelope, while maintaining the narrower band spectral signatures of the target vapor cloud. The broad band suppression requires three steps. First, selection is made of an interferogram segment where the narrow band target signature remains relatively strong compared to the attenuated broad band background signal.[11] Second, a bandpass digital filter is applied to the selected interferogram segment to remove signals at

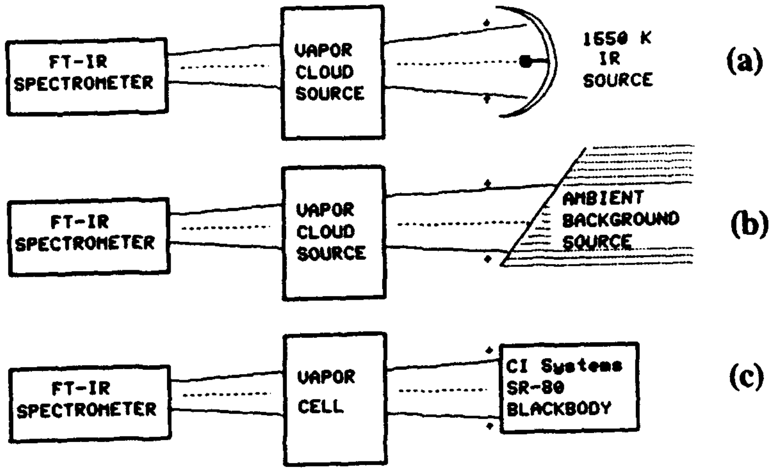

Figure 1. Experimental Methods for Data Collection:
(a) Active Bistatic, (b) Passive Terrestrial, and
(c) Passive Laboratory Spectrometer Configurations.

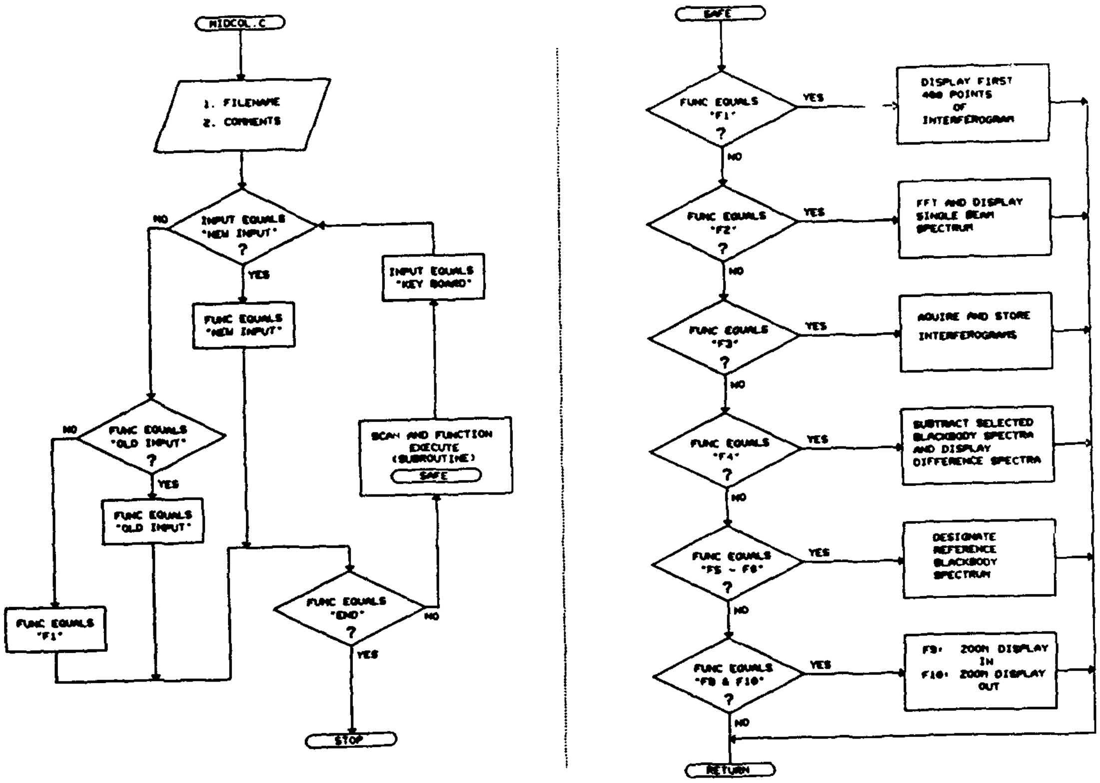

Figure 2. Flow Chart of the Data Collection Program.

frequencies other than those corresponding to a selected band of the target vapor. Third, pattern discrimination techniques are applied to the filtered interferogram segment. These discrimination techniques effectively examine the narrow band shape of the target vapor to avoid erroneous detections due to interferant vapors. The three step background suppression process is demonstrated for two VOCs (i.e., acetone and methyl ethyl ketone) as well as a narrower band test gas (i.e., sulfur hexafluoride). Interferogram data is collected under a variety of experimental conditions to evaluate the effectiveness of the three step background suppression technique.

2. INSTRUMENTATION

The MIDAC FT-IR emission spectrometer (serial number 120) with a Newtonian telescope and remote IR source is used in this investigation (Midac, Inc., Irvine, CA). The FT-IR spectrometer consists of a linear drive Michelson interferometer with a germanium coated zinc selenide beamsplitter/compensator plate. An off-axis parabolic mirror focuses the IR radiation onto a 2×2-mm liquid nitrogen cooled Hg:Cd:Te detector that is designed for 8 to 12 micron response. The spectrometer is found to possess a 6° field of view (FOV).[‡] The Newtonian telescope provides a limited 0.3° (FOV) with a 500 cm^2 aperture which can be filled with the IR source. The IR source is composed of a 2000 cm^2 aperture metal paraboloid to collimate a 1550 K silicon carbide heater element point source. The interferometer scan speed is established to be 2.454±0.005 mm/sec for these measurements.[12,13] The interferogram data is sampled at every eighth zero crossing for a total of 1024 sampled points. Spectra that are computed from these interferograms have a spectral point spacing of approximately 4 cm^{-1}.

The spectrometer is interfaced to a Dell System 486P/50 IBM PC compatible computer operating under MS-DOS Version 5.0 (Microsoft, Redmond, WA). Interferogram collection is performed with the MIDCOL software package.[14] This software is written in Microsoft C, Version 6.1 and utilizes graphics routines from Essential Graphics System (South Mountain Software, Inc., Orange, NJ). The program permits rapid data collection of interferograms in 16-bit integer format as delivered from the spectrometer's analog-to-digital converter. Figure 2 provides a flow chart of the data acquisition portion of the MIDCOL software and outlines its functions. The MIDCOL software places interferograms into

---

[‡]Tveten, L.H., "Acceptance Test Procedure for the Background Measurement Spectroradiometer," Technical Report CDRL Seq. No. A019, ATP 25368-01, DAAK-79-C-0051, Honeywell Inc., St. Petersburg, FL, October 1979.

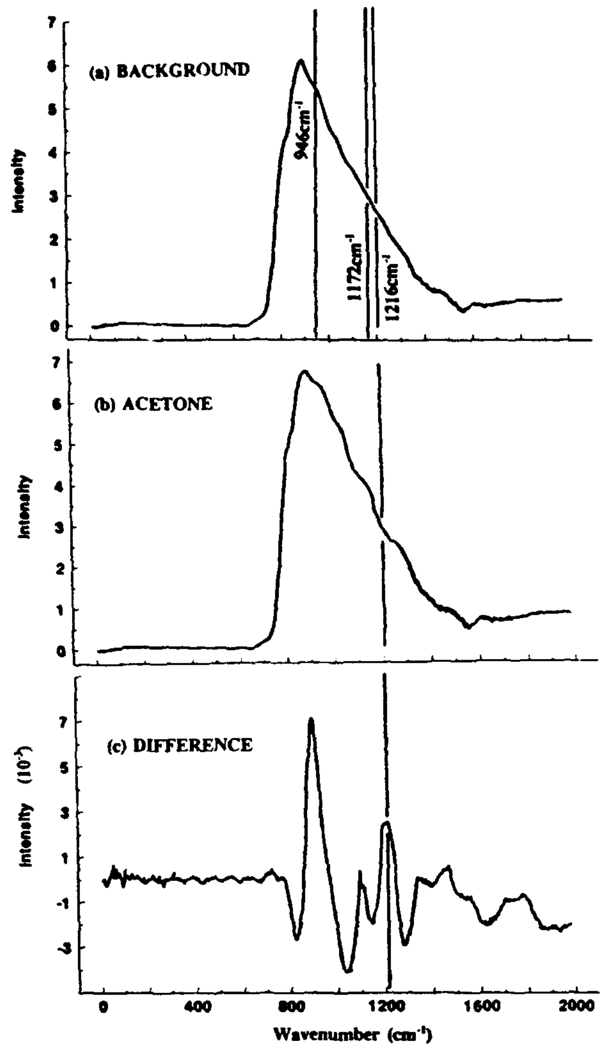

Figure 3.

Single-Beam Passive Terrestrial Spectra with Comparable Responses: (a) Background, (b) Acetone, and (c) Acetone/ Background Difference.

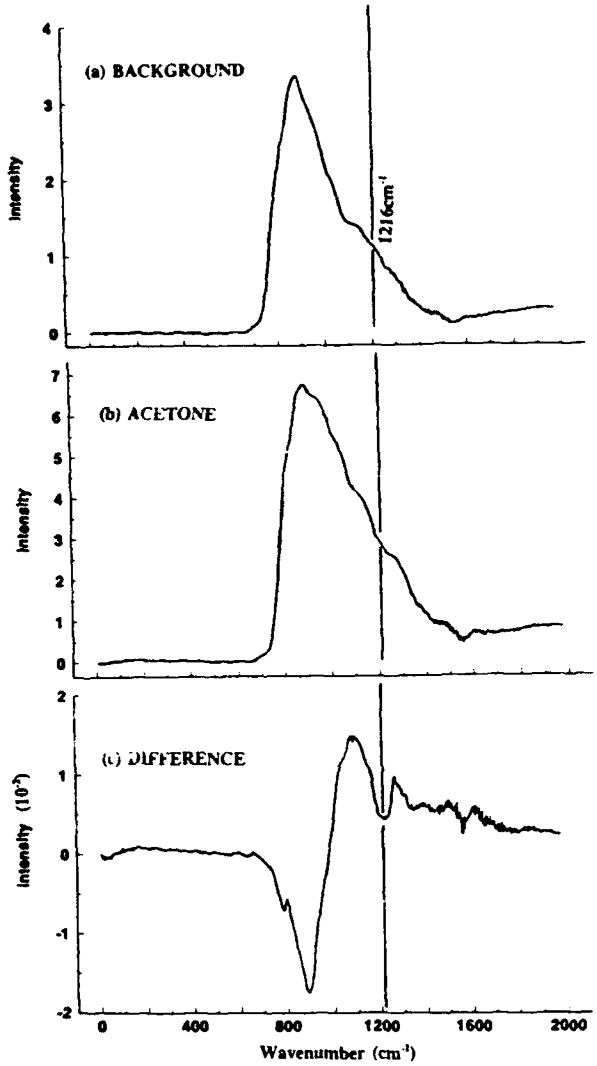

Figure 4.

Single-Beam Passive Terrestrial Spectra with Dissimilar Responses: (a) Background, (b) Acetone, and (c) Acetone/ Background Difference.

aggregate data files that are composed of up to 3000 interferogram subfiles. The data files are prefixed with a global header which contains filename, date, time of day, interferometer configuration, meteorological data, comments, and number of interferogram subfiles. Each interferogram subfile is identified by a subfile header which includes scan number, time of day, center burst location, and error code. This header information allows a systematic labeling and categorization of the data important in subsequent data analysis. Appendix A contains the file format specifications.

3. EXPERIMENTAL METHODS

The limit of detection for remote FT-IR spectrometers is governed by four parameters: (1) radiance difference between IR background source and target vapor, (2) vapor path length, (3) vapor concentration, and (4) atmospheric attenuation. These parameters are present for all three experimental methods that are used in this investigation (see Figure 1). The active bistatic configuration, shown in Figure 1a, provides an IR source of such intensity that the lower vapor radiance becomes insignificant. A transmission experiment is performed when the IR source is operated at 1550 K. Distances from the IR source to the FT-IR spectrometer varied from 25-100 meters. In the bistatic configuration, variations of the vapor cloud concentration and atmospheric attenuation control the limit of detection.[4,7] If the IR source temperature is significantly reduced and/or the IR source does not fill the spectrometer FOV, then the IR source radiance becomes comparable to that of the vapor. Under these conditions, the spectral response of the bistatic configuration resembles that of the passive approach.

The passive terrestrial approach is described in Figure 1b and uses only the ambient background terrain radiance. The 1550 K IR source provides an initial alignment and is subsequently removed from the spectrometer FOV. In the passive case, the radiance difference between the ambient background (i.e., about 300 K) and the target vapor is often small. This small radiance difference is usually the controlling factor in detection. If the contrast radiance between the vapor cloud and terrain background is insufficient, then no spectral target vapor detection is possible.[6,15] For the bistatic and passive configurations, VOC vapors have been dispensed by either static or forced air flow evaporation of spectral grade Aldrich chemicals. Sulfur hexafluoride (SF_6) releases have been made with a fixed flow rate from a Matheson Gas Products QA gas cylinder.[16]

The third and final approach in Figure 1c experimentally simulates the passive terrestrial measurements in the laboratory. The telescope is not used in this experiment. The

Table 1. Interferogram Origin and Usage Summary.

		COLLECTION SETS		TRAINING SET		PREDICTION SET	
		TRAINING	PREDICTION	VAPOR	BACKGROUND	VAPOR	BACKGROUND
ACTIVE BISTATIC	Acetone	4998	8250	850	1546	2737	1168
	MEK	4998	8250	1121	1886	33	1985
	SF_6	4982	6050	211	2192	0	1800
PASSIVE TERRESTIAL	Acetone	14626	18950	89	6016	2100	3881
	MEK	14076	20900	103	5282	954	3061
	[illegible]	13848	10274	57	5803	0	4027
PASSIVE LABORATORY	Acetone	3886	18778	84	1415	63	51
	MEK	3886	19654	74	1534	2363	1604
	SF_6	6584	10800	660	1077	1933	2240

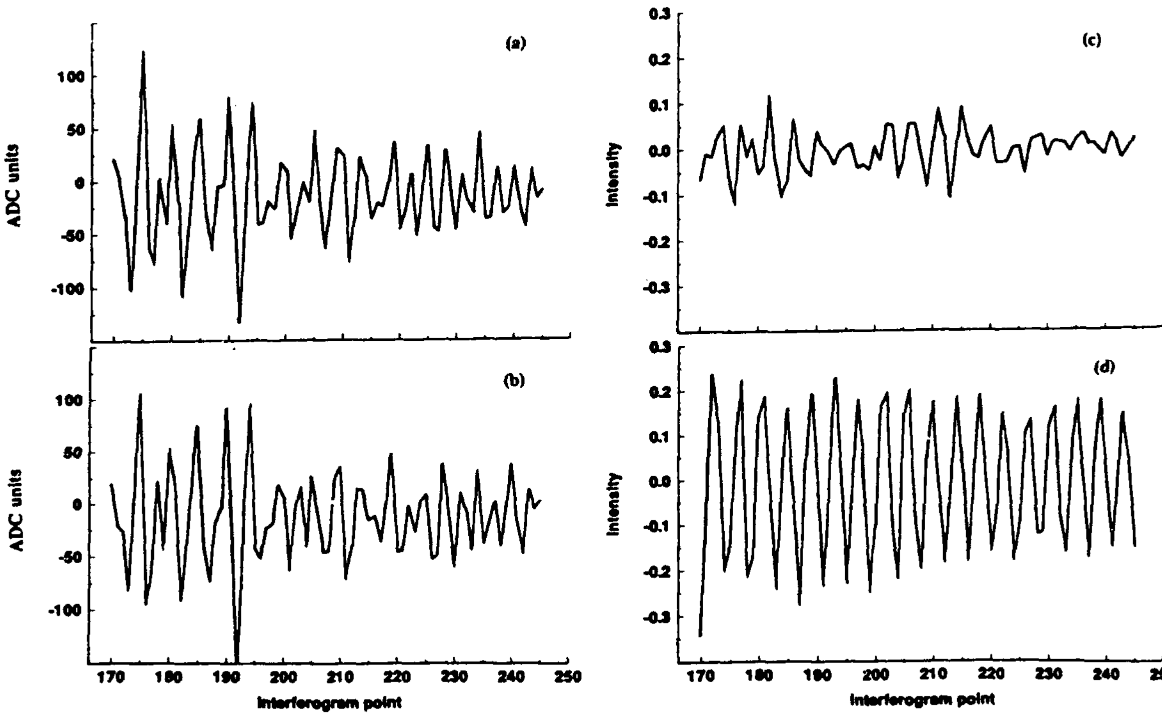

Figure 5. FIRM Filter Response for Raw Interferogram Segments with and without SF_6 Present.

vapor source is a small aperture and short path length vapor cell.[17] The short path vapor cell provides an aperture of 62 cm^2 and a path length of 8.2 cm. The 4×4-inch extended SR-80 blackbody[18] furnishes an adjustable temperature source from 5 to 50 °C. The blackbody is a NIST traceable source that is accurate to ±0.03 °C and precise to ±0.01 °C. The optical train of FT-IR spectrometer, vapor cell, and blackbody is aligned with a helium neon laser. Distances between spectrometer/cell and cell/blackbody are approximately 10 cm. These distances along the optical train axis ensure that the spectrometer FOV lies within the 62 cm^2 aperture of the short path cell and views only the 4×4-inch blackbody IR background.

A variety of conditions are used in data collection with the spectrometer configurations of active bistatic, passive terrestrial, and passive laboratory that are illustrated in Figure 1. Table 1 summarizes the number of interferograms collected with each configuration for each target vapor. Separate training and prediction data sets of interferograms have been acquired for each vapor (see Table 1). The training set interferograms are used in selection of the appropriate interferogram segment, computation of the optimal bandpass digital filter, and optimization of the pattern discrimination procedures. The prediction set interferograms serve as an independent test set for evaluation of the background suppression procedure. The complete training set contains 23510 interferograms for acetone, 22960 interferograms for MEK, and 25414 interferograms for SF_6. The complete prediction set holds 45978 interferograms for acetone, 48804 interferograms for MEK, and 27124 interferograms for SF_6. The representative background interferograms for the training and prediction subsets of each vapor are determined by the global sampling algorithm developed by Carpenter and Small.[19] Numbers of interferograms, that are selected, are listed in Table 1. Approximately 1000 interferograms for the training subsets of each compound are selected on the basis of visual inspection of the Fourier transformed spectra (see Appendix B for types of interferograms selected). Similarly, a number of vapor containing interferograms are selected for the prediction subsets giving a total of 10000 interferograms in each subset. The passive laboratory interferograms have provided an accurate test to verify the visual inspection of spectra for conditions near the spectrometer's detection limit.

4. ANALYSIS

4.1 Frequency-Domain Analysis.

Spectral analysis for vapors in the IR depends on the parameters of band position, width, strength and contour. Table 2

summarizes both the spectral[20,21,22] and vapor pressure[23] information pertinent to the vapors that have been investigated in this study. Columns three and four of Table 2 contain the absorptivities and vapor pressures. These provide an estimate of relative band intensities assuming an uniform detector response. Unfortunately, photoconductor detectors usually possess an uniform response over very limited spectral ranges as demonstrated in Figure 3a for a single-beam passive background spectrum. The band positions for the VOCs and SF_6 are also delineated in the background spectrum of Figure 3a and tabulated in column one of Table 2. The band widths are listed in column two of Table 2 as the full-width-at-half-height (FWHH) values. A band overlap of about 100 cm^{-1} occurs between acetone and methyl ethyl ketone (MEK). In addition, the detector response for these VOC band positions is only about one half that of the SF_6 band position.

The lower detector response combined with a decrease in the VOC absorptivity by a factor of 20 to 40 as compared to SF_6 makes the detection of VOCs much more difficult than SF_6. The detection is further complicated by variation of the background for passive terrestrial measurements. Figures 3 and 4 show the difference between an acetone spectrum and two separate background spectra. The background and acetone spectra in Figure 3 are collected under similar conditions. The difference spectrum contains a prominent acetone feature. Measurement of another background only a few minutes later shows a substantial change in the background radiance has occurred. In this difference spectrum (see Figure 4c), the acetone feature becomes hidden by a large baseline fluctuation. This emphasizes the potential problem with attempts of averaging consecutive spectra to increase the signal-to-noise ratio (SNR). For spectra with low SNRs, the background variation also limits the utility of the traditional approach of a reference background subtraction followed by classification with a linear discriminant.[6] Unfortunately, it is often impossible to obtain an accurate reference background spectrum. Therefore, an alternate method of background removal or suppression is necessary for this application.

4.2 Time-Domain Analysis.

The superposition of a set of damped cosine waves describes an IR interferogram. The set of damped cosine waves is defined by the IR radiation detected with the spectrometer. The cosine damping for each frequency defines the composition of frequencies distributed across the interferogram.[11] A large damping factor indicates a wide band in the frequency domain, while a small damping factor corresponds to a narrow band. Both the digital filtering and the Gram-Schmidt vector orthogonalization[24] procedures for direct interferogram analysis

rely on the broad band of the detector response damping out before the narrow band of the target compound. This effect results in the selection of interferogram segments that are displaced from the zero path difference (ZPD) of the interferogram center burst.[24,25,26] A comparison of the digital filter and Gram-Schmidt approaches by Bjerga and Small[26] indicates that the digital filter achieves a lower SNR detection and provides enhanced computational efficiency. Therefore, the digital filter approach is used for the remote monitoring of acetone and MEK which have SNRs significantly lower than SF_6. The generation of the digital filter requires the judicious selection of both the filter type and interferogram segment. Subsequent examination of the digitally filtered interferogram segments with pattern recognition techniques furnishes a discrimination capability which depends on the spectral band contour of the target vapor.

Table 2. Spectral and Vapor Pressure Information

	$\bar{\nu}_{peak}$ (cm^{-1})	FWHH $\Delta\bar{\nu}_{bw}$ (cm^{-1})	$a(10^4)$ (m^2/mg)	P_{vap}@21°C (mm of Hg)
Acetone	1217[20,22] 1216†	49†	1.3[20] 2.0[22]	193.9[23]
MEK	1175[20] 1172†	29†	0.5[20]	74.5[23]
SF_6	939[21] 947[22] 946†	10†	47.9[22]	[1.7(10^4) GAS][16]

† From MIDAC spectrometer operated at 4 cm^{-1} resolution.

4.2.1 Digital Filtering.

Digital filtering is a standard means of removing unwanted noise frequency components by smoothing.[27] Digital filters also provide the ability to remove other selected interference frequencies.[28] The most common type of digital filter for selective frequency attenuation is the finite-impulse-response (FIR) filter. Equation 1 is the functional form of the FIR filter.

$$Y_i^* = f_1 \bullet Y_{i-N} + \ldots. + f_{N+1} \bullet Y_i \quad (1)$$

Y_i^* denotes the resultant filtered data point. Y_{i-N} to Y_i represent the input unfiltered data points. The coefficient weights, f_1 to

f_{N+1} determine the filter's frequency response. If each coefficient weight is set to $1/(N+1)$, then a moving average results. The moving average filter has a low pass frequency response. Digital filtering for the extraction of specific spectral bands in interferograms requires a response that depends on both the spectral band and detector response curve.

A FIR filter has previously been developed to extract the SF_6 spectral feature at 940 cm^{-1} from interferograms collected with a passive FT-IR spectrometer mounted on a helicopter.[6,9] The derivation of the filter coefficients begins in the frequency domain. First, a multiplication of a Gaussian function with the spectrum containing SF_6 is performed. The Gaussian function is centered on the SF_6 band at 940 cm^{-1} and possesses a bandwidth of 14 cm^{-1}. The multiplication results in an ideal filtered spectrum. The inverse Fourier transform provides the filtered interferogram. To perform the filtering function in the time domain, this investigation uses equation 1. Equation 1 is a linear model that relates the set of independent variables (raw interferogram points) and dependent variable (filtered interferogram points). The coefficient weights are determined by regression analysis on a set of interferograms containing SF_6. The constraint is imposed on the regression analysis that consecutive interferogram points must be used in generation of each filtered interferogram point.

Subsequent work has focused on removal of the constraint requiring that each filtered interferogram point use the same number of consecutive raw interferogram points.[11] This permits a different filter model to be used for each point. A stepwise multiple regression permits identification and deletion of the filter coefficient terms that are less significant in approximation of the ideal filtered interferogram. This type of filter is called a finite impulse response matrix (FIRM) filter. The fewer filter coefficient terms of the FIRM filter for a given interferogram point reduces the dynamic range requirements that are placed on the filter coefficients. This has given an improved performance in computational efficiency and SNR enhancement.

This investigation used FIRM filters. The optimal interferogram segment location for the narrow band SF_6 was a 75 point segment that was 170 interferogram points displaced from the ZPD. A FIRM filter was generated using this segment for the training set of 928 interferograms containing SF_6 and 9072 background interferograms. The percentage distribution of interferograms from the active bistatic, passive terrestrial, and passive laboratory configurations was 24:59:17 respectively (see Table 1 columns 3 and 4). Coefficient terms were selected from points i-0 to i-100 in equation 1 using stepwise regression. The entrance criterion for coefficient term inclusion in the filter was at a significance level of 99.99% based on the F test. The

average R^2 value for the regression calculations was 99.0% and the average number of coefficients required to filter each point was thirty.

The application of the FIRM filter is illustrated in Figure 5. The Figures 5a and 5b are plots of raw interferogram segments, while Figures 5c and 5d are plots of the corresponding FIRM filtered segments. Figures 5a and 5c show the effect of the filter on a background interferogram segment with SF_6 absent. Figures 5b and 5d demonstrate the filtered response when SF_6 is present in the raw interferogram segment. Clearly, Figure 5 illustrates the effectiveness of the FIRM filter in extracting the narrow band SF_6 spectral feature from the raw interferogram segment.

4.2.2 Pattern Recognition Considerations.

The identification of a specific IR vapor signature is often made using a pattern recognition method known as linear discriminant analysis. The linear discriminant classifies a FT-IR interferogram on the basis of the presence or absence of a specific spectral signature. The linear discriminant is described by equation 2.[29]

$$g(x) = w_o + \sum_{i=1}^{N} w_i \bullet x_i \tag{2}$$

The w_i term denotes a weight vector. The response vector is represented by x_i term. The w_o term is a threshold vector. The g(x) term is the spectral response function. The linear discriminant, equation 2, divides the feature space with a hyperplanar surface. Thus, the weight vector has a number of dimensions that are defined by the interferogram points. Determination of the weight vector requires using a representative training data set. The training set is separated with an optimum weight vector by using a convergence technique based on the perceptron convergence theorem. This vector gives a minimum response to spectral interferants and a maximum response to the target vapor. The perceptron convergence theorem uses an iterative approach to determine the weight vector. It begins by locating all misclassifications. These misclassifications are used to estimate a new weight vector. The process continues until all the data are correctly classified or it is assumed that the data set is linearly inseparable.

The constraint of linear separability is often too limiting. The present study uses a technique called piecewise linear discriminant analysis (PLDA).[30] This technique uses pieces or portions of several linear discriminants (i.e., multiple linear discriminant) to approximate a nonlinear surface that

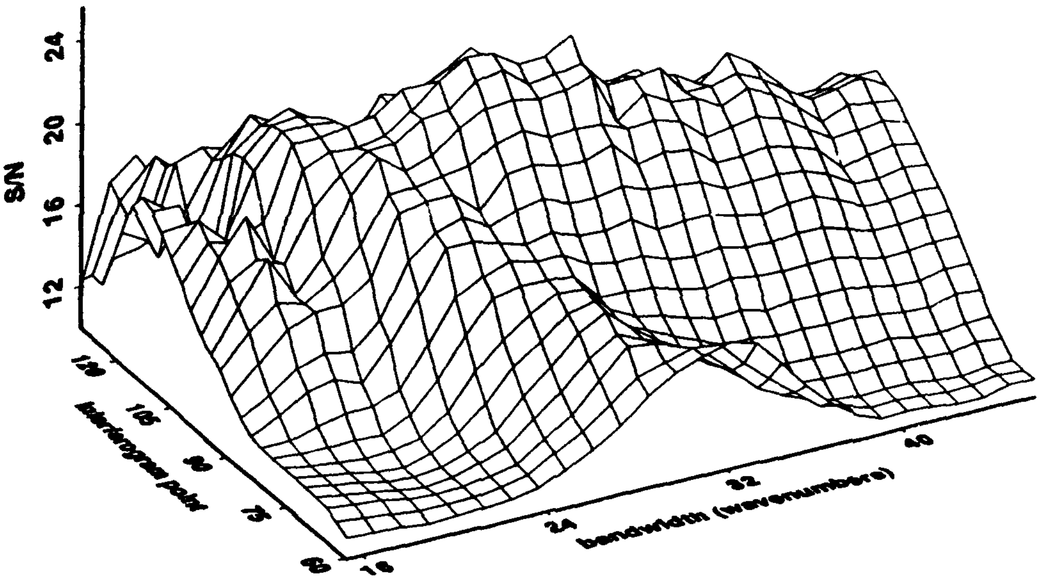

Figure 6. FIRM Filter S/N Variation with Interferogram Segment Location and Gaussian Peak Position.

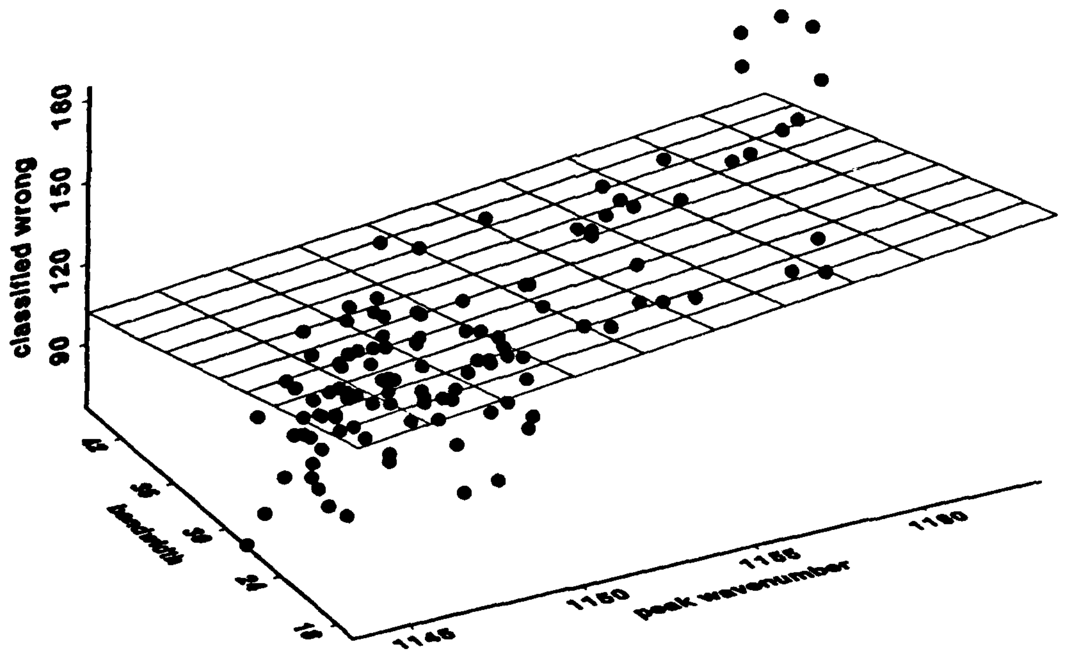

Figure 7. Incorrect Classifications for the Multilinear Discriminant with Various Gaussian Band Widths and Peak Positions.

better classifies the interferogram in pattern space. The PLDA approach also incorporates a simplex optimization for a more effective placement of the individual linear discriminants.

4.2.3 Digital Filter Design.

Digital filter and pattern recognition coefficients have been generated for acetone, MEK, and SF_6. The most intense spectral band for each vapor in the 8-12μm atmospheric window has been used in the filter design (see Table 2, column 1). A description is given below for the three steps necessary to generate robust sets of coefficients. The coefficients are vapor specific. Description of the procedure uses only MEK, since the same technique applies to each vapor. Results of the procedures that are used for acetone and SF_6 are contained in Appendix C.

The first step was to acquire a representative subset from the 22960 interferograms in the full training set. This training subset contained 10000 interferograms which included 1298 vapor containing interferograms and 8702 background interferograms. The training subset selection was made with the global sampling algorithm developed by Carpenter and Small.[19] A tally of the types of interferograms that were placed in the training subset is provided in Table 1.

The second step was generation of the FIRM filter coefficients. Smaller subsets of about 400 interferograms were selected from the 1298 vapor containing interferograms in the training subset. The FIRM filter coefficients were generated according to the techniques described by Small and Harms.[11] Input parameters important to the performance of the filter included interferogram segment length, interferogram segment location, the Gaussian bandpass function peak position, and the Gaussian bandpass function FWHH. The Gaussian function as noted previously was used to produce the ideal filtered spectrum. In this investigation only the filtered interferogram segment length was held constant at 75 interferogram points. The 75 point segment was shown optimal for SF_6.[11] The VOCs with wider spectral band widths (see Table 2, column 2) might be optimal with shorter interferogram segment lengths (i.e., lower resolution). Further investigation is required to test this hypothesis.

The third step was to determine the optimum for the three remaining filter parameters. Sets of 759 different FIRM filters for different Gaussian peak positions were generated over a range of interferogram segment locations and band widths. To assess the digital filter performance before attempting to perform a PLDA, a one-dimensional discriminant was computed for identifying potentially effective filters. The different intensity responses of the filtered interferogram segments in Figures 5c and 5d suggested that the sum-of-squares (SOS) of the

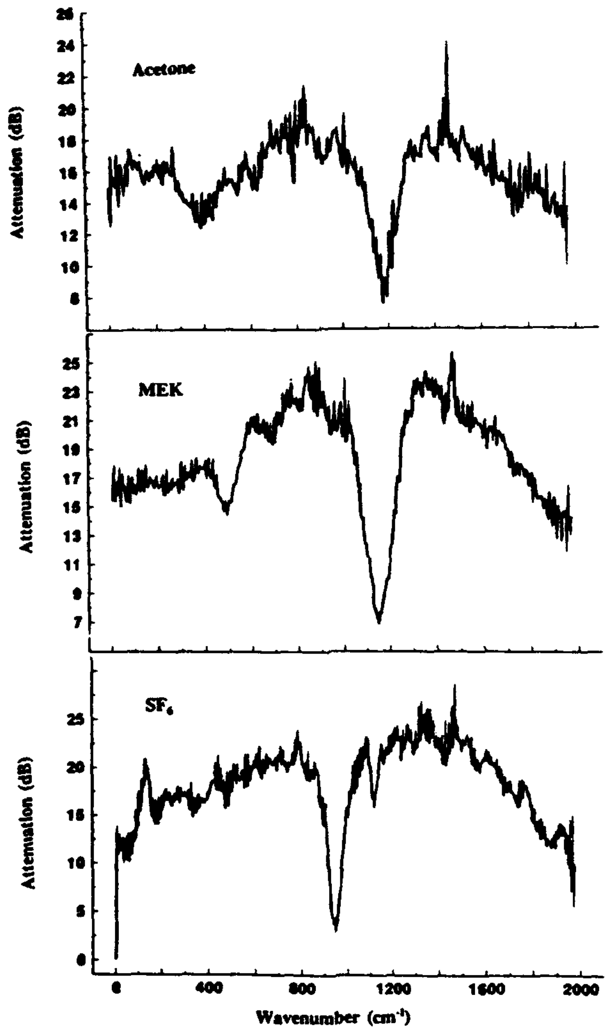

Figure 8. FIRM Filter Frequency Response.

filtered interferogram points would provide such a one-dimensional discriminant. Separate average magnitude responses were found with the SOS calculation for subsets of the vapor and background interferograms in the training set (see Table 1). The ratio of vapor to background averaged responses is denoted as the signal-to-noise ratio (S/N). A three dimensional plot of the S/N for varying interferogram segment locations and Gaussian function band widths is shown in Figure 6. The axis for interferogram segment locations is labeled with the starting point in the segment closest to the interferogram ZPD. The maximum S/N in Figure 6 was an interferogram segment location displaced 105 points from the ZPD and a Gaussian function band width greater than 24 cm^{-1}. The fourth dimension, the Gaussian peak location, was not shown in Figure 6. The Gaussian peak location of 1150 cm^{-1} was used in this plot. This particular Gaussian peak was subsequently found to produce the lowest number of misclassified interferograms when a PLDA was performed. Thus, the filter coefficients were de facto selected by the same criterion of lowest misclassifications. Multiple linear discriminants were generated with the PLDA approach.[30] The number of interferograms classified incorrectly out the training set of 10000 interferograms is shown in Figure 7 as a function of Gaussian peak position and band width. The lowest number of incorrect classifications was for a peak position of 1150 cm^{-1} and band width of 27 cm^{-1}. These results are for a 75 point segment displaced 105 points from the interferogram ZPD. These findings along with those for acetone and SF_6 are summarized in Table 3.

Table 3. Optimal Filter Response Parameters

	INTERFEROGRAM POINT SEGMENT LOCATION	GAUSSIAN PEAK POSITION (cm^{-1})	GAUSSIAN BANDWIDTH (cm^{-1})	FILTER PEAK RESPONSE (cm^{-1})
ACETONE	80 - 155	1195	31	1190
MEK	105 - 180	1169	27	1150
SF_6	170 - 245	941	14	945

5. RESULTS AND DISCUSSION

The performance of the digital filter and multiple linear discriminant is best evaluated with the results obtained from a separate prediction set of interferograms. Table 1 lists the number of interferograms that have been obtained with the spectrometer configurations of active bistatic, passive

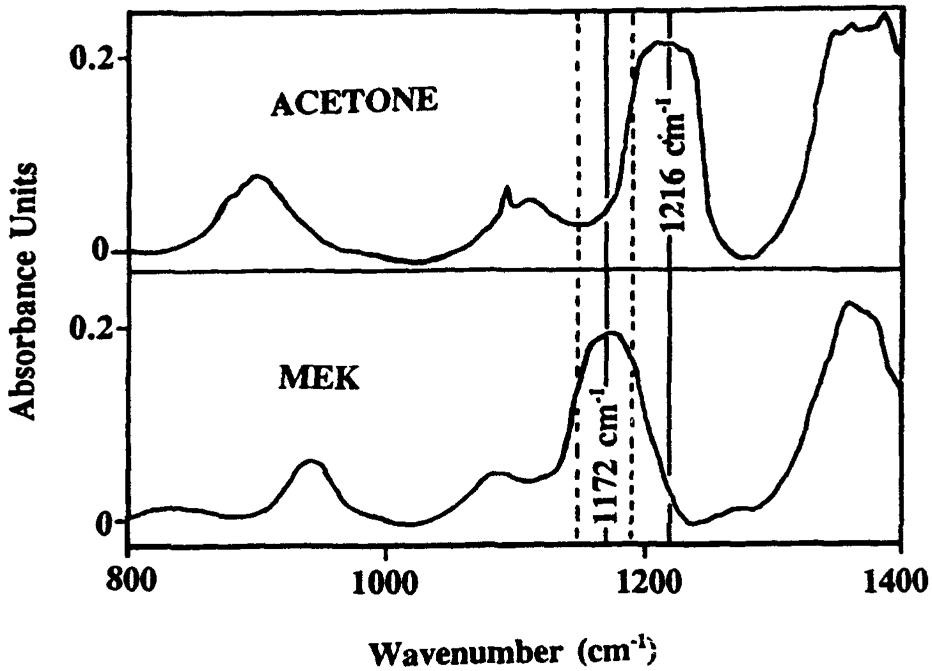

Figure 9. Absorbance Spectra with Active Bistatic Spectrometer Configuration.

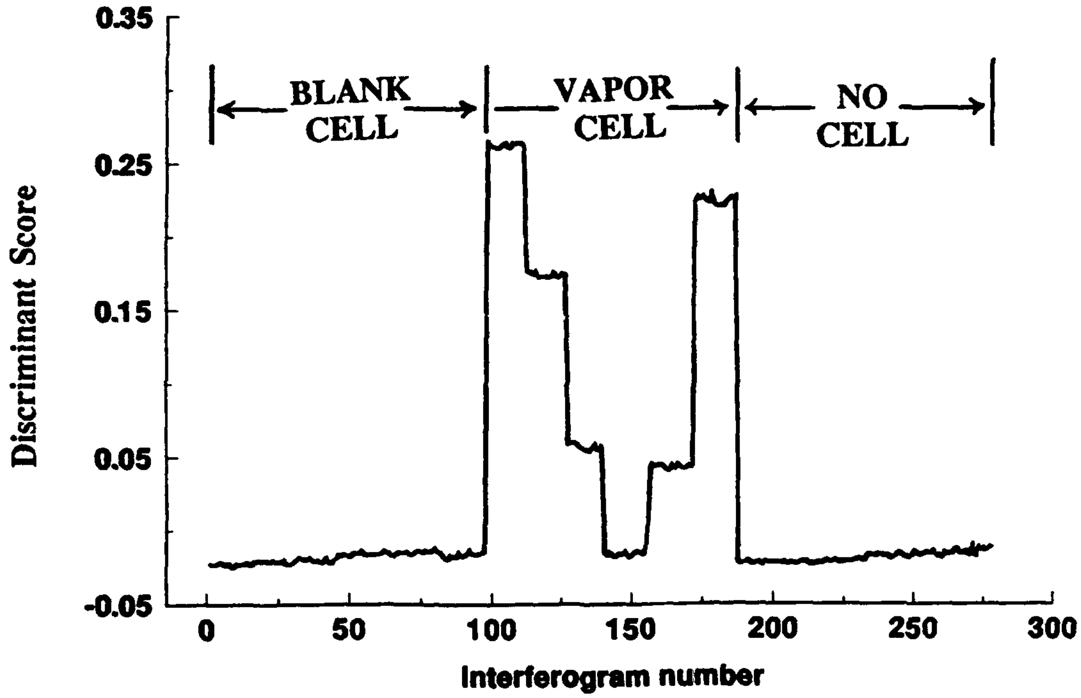

Figure 10. Discriminant Scores for the Passive Laboratory Spectrometer Configuration.

terrestrial, and passive laboratory for the prediction test set. The classification results for the digital filter and multiple linear discriminant are summarized in Table 4. Two types of misclassifications or incorrect alarms occur. A false alarm occurs when no vapor is present, but the digital filter and multiple linear discriminant indicates a positive detection. A missed alarm results for no detection when the vapor is actually present. The percentages for false and missed alarms are determined from the ratios of misclassifications to backgrounds and vapor containing interferograms respectively (reference Table 1 for denominator values in ratio). The false alarms on the training set are set to zero as a computational constraint. The acetone and MEK results are comparable for missed alarms. The slightly higher percentage for missed alarms in the prediction set is to be expected. However, the false alarm percentage, though reasonable for acetone is about an order of magnitude higher for MEK and comparable in magnitude to the missed alarms. If vapor containing interferograms are incorrectly classified in the training set then a higher false alarm count results. A closer examination of the training set is required to test this possibility.

The classification results for SF_6 are also listed in Table 4. The number of interferograms are listed in Table 1 that are selected for training and prediction subsets. These subsets differ in that the prediction subset contains only passive laboratory data for the vapor-present case. On the other hand, the SF_6 training subset includes interferograms from all three spectrometer configurations for the vapor-present case. Using only the passive laboratory data for the prediction subset provides a more accurate determination of the causes for false or missed alarms. The number of false alarms for SF_6 is comparable to MEK. However, closer examination of the data reveals about 20 of the 25 false alarms are made for conditions near or less than the detection limit of the spectrometer. Using a reference blackbody background subtraction indicates that only about 5 of the 20 false alarms are valid. Therefore, a more realistic count of false alarms is 10 (i.e., 0.5%).

The FIRM filter parameters are given in Table 3. These parameters have been used in the generation of the Table 4 classification results. A plot of the FIRM filter frequency responses is shown in Figure 8. The frequency response plots are generated with the approach that is given in Appendix D. The attenuation provided by the FIRM filters is consistent with the signal dynamic range. For interferogram segments displaced off the interferogram center burst only about nine bits of the analog-to-digital converter range is used. Therefore, a filter attenuation in excess of about 27 decibels (dB) is unnecessary. The attenuation in the filter bandpass removes the residual broad band detector envelope. Hence, the bandpass attenuation

becomes greater as the interferogram segment location approaches the interferogram center burst region. The gradual decrease of attenuation away from the filter bandpass reflects the inherent optical filtering of the detector response curve (i.e., detector cutoffs near 800 cm^{-1} and 1600 cm^{-1}).

Table 4. Classification Results

		FALSE ALARMS	MISSED ALARMS	TOTAL CORRECT
TRAINING RESULTS	Acetone	0 (0.0%)	27 (2.6%)	9973 (99.7%)
	MEK	0 (0.0%)	63 (4.8%)	9937 (99.4%)
	SF_6	0 (0.0%)	11 (1 2%)	9989 (99.9%)
PREDICTION RESULTS	Acetone	16 (0.3%)	268 (5.5%)	9716 (97.2%)
	MEK	259 (3.9%)	201 (6.0%)	9540 (95.4%)
	SF_6	25 (1.3%)	89 (1.1%)	9886 (98.9%)

The optimal FIRM filter and multiple linear discriminant performance occurs for the minimum in classification errors for the training subset. The optimum for the VOCs gives a minimum error classification count for a filter response curve centered off the spectral band. The peak filter bandpass responses differ from the acetone and MEK spectral bands by 26 cm^{-1} and 22 cm^{-1} respectively. No such difference is discernible for the SF_6 filter response. The SF_6 case, unlike the VOCs does not possess a lower intensity band adjacent to the major spectral feature. This lower intensity band becomes important for the bistatic active spectrometer configuration. Figure 9 shows the absorbance spectra for acetone and MEK that is taken in the active bistatic spectrometer configuration. The peak spectral positions are delineated with solid lines, while the broken lines indicate the peak filter pass band response. It is important to note that the digital filtering of the short interferogram segment is only one step in the background suppression method. The classification is made with the multiple linear discriminant that is generated by PLDA[30] on the filtered interferogram segment. The multiple linear discriminant uses pertinent band contour

information that facilitates a separation in the pattern space. In the VOC case, frequency components from the lower intensity band that is adjacent to the major spectral band become important. These results indicate that more work is needed to assess the importance of functional filter forms other than the Gaussian for direct interferogram processing.

The VOC FIRM filter and multiple linear discriminants have been implemented on an IBM/PC compatible computer.[14] The results of the real-time operation with the MIDAC spectrometer is shown in Figure 10. Figure 10 is a plot of the multiple linear discriminant score as a function of sequentially collected interferograms. These interferograms are collected in the passive laboratory spectrometer configuration. A fixed concentration of MEK is contained in the vapor cell. The blackbody background temperature is varied around the cell ambient temperature by approximately 5°C increments for a blank cell, vapor cell, and no cell. The distribution of interferograms are as follows: 0-97, blank cell background; 98-187, vapor cell; and 188-278, no cell. The background and vapor cell temperatures are equal for interferograms 141 to 155. The discriminant performs as expected with no response for interferograms 141 to 155. Clearly, a nonzero temperature differential between the vapor and the background is required to produce a spectral emission or absorption vapor spectrum.

6. CONCLUSIONS

The application of FIRM filters on selected interferogram segments followed by a multiple linear discriminant analysis provides a means of suppressing the broad band detector envelope. This removes the need for a stable reference background spectrum. Often a background reference spectrum does not exist for many open-air monitoring conditions, especially with passive terrestrial spectrometer configurations. The background suppression approach is found to work well in the discrimination for the vapors studied, while rejecting spectral information from other atmospheric constituents. This discrimination capability is essential for many atmospheric monitoring applications.

Acetone, MEK, and SF_6 provide spectral bands of decreasing bandwidth. These bandwidths are shown to relate directly to the optimum interferogram segment selected for digital filtering with the broader bands residing nearer the center burst. The multiple linear discriminant analysis has clearly demonstrated the importance of band contours when contrasting the results for the VOCs versus SF_6. Direct processing of interferograms with digital filtering combined with multiple linear discrimination facilitates the use of FT-IR spectrometry in open-air monitoring applications.

Blank

LITERATURE CITED

1. Dublin, T., and Thone, H.J., "Quantitative Analysis of Organic Multicomponent Mixtures of Gases and Vapors in Industrial Air Emissions by IR-Spectrometry," Fresenius Z. Anal. Chem. Vol. 335, pp 279-285 (1989).

2. Chan, C.C., et al., "Driver Exposure to Volatile Organic Compounds, CO, Ozone, and NO_2 under Different Driving Conditions," Environ. Sci. Technol. Vol. 25(5), pp 964-972 (1991).

3. Berkley, R.E., Varns, J.L., and Plell, J., "Comparison of Portable Gas Chromatographs and Passivated Canisters for Field Sampling Airborne Toxic Organic Vapors in the United States and USSR," Environ. Sci. Technol. Vol 25(8), pp 1439-1444 (1991).

4. Spartz, M.L., et al., "Evaluation of a Mobile FT-IR System for Rapid Volatile Organic Compound Determination, Part I: Preliminary Qualitative and Quantitative Results," Amer. Environ. Lab. Vol 21(2), p 15 (1989).

5. Herget, W.F., "Remote and Cross-Stack Measurement of Stack Gas Concentrations Using a Mobile FT-IR System", Applied Optics Vol. 21(4), pp 635-641 (1982).

6. Kroutil, R.T., Ditillo, J.T., and Small, G.W., "Signal Processing Techniques for Remote Infrared Chemical Sensing," In Computer Enhanced Analytical Spectroscopy, Vol. 2, pp 71-111, Ed. H. Meuzelaer, Plenum Pub. Corp., New York, NY, 1990.

7. Carter, R.E., et al., "A Method of Predicting Point and Path-Averaged Ambient Air VOC Concentrations Using Meteorological Data," J. Air. Waste Manage. Assoc. Vol. 43, pp 480-488 (1993).

8. Hudson, R.D., Jr., Infrared System Engineering, pp 35-50, John Wiley & Sons, New York, NY, 1969.

9. Small, G.W., Kroutil, R.T., Ditillo, J.T., and Loerop, W.R., "Detection of Atmospheric Pollutants by Direct Analysis of Passive Fourier Transform Infrared Interferograms," Analytical Chemistry Vol. 60(3), pp 264-269 (1988).

10. Small, G.W., Kaltenbach, T.F., and Kroutil, R.T., "Rapid Signal Processing Techniques for Fourier Transform Infrared Remote Sensing," Trends in Analytical Chemistry Vol. 10(5), pp 149-155 (1991).

11. Small, G.W., Harms, A.C., Kroutil, R.T., Ditillo, J.T., and Loerop, W.R., "Design of Optimized Finite Impulse Response Digital Filters for Use with Passive Fourier Transform Infrared Interferograms", Analytical Chemistry Vol. 62(17), pp 1768-1777 (1990).

12. Combs, R.J., and Cathey, C.T., "Measurement of a Michelson Interferometer Mirror Velocity," Analytical Instrumentation Vol. 20(4), pp 223-256 (1992).

13. Combs, R.J., Knapp, R.B., and Field, P.E., "Mirror Velocity Errors in a Michelson Interferometer," Analytical Instrumentation, in press.

14. Kroutil, R.T., Housky, M., and Small, G.W., "Real-Time Data Collection Programs for a Commercial Passive FT-IR Remote Sensor," Spectroscopy, in press.

15. Chandrasekhar, S., Radiative Transfer, Dover, New York, NY, 1960.

16. Braker, W., and Mossman, A.L., Matheson Gas Data Book, 3rd Printing, p 649, Matheson Gas Products, NJ, 1980.

17. Combs, R.J., and Knapp, R.B., "Response Time of a Short-Scan Interferometer for Stand-off Detection of Chemical Agents," CRDEC-TR-387, U.S. Army, Chemical Research, Development, and Engineering Center, Aberdeen Proving Ground, MD, July 1992, Unclassified Report.

18. SR-80 Extended Area Infrared Radiation Source, 550-490-0010, C.I. Sys. Inc., Agoura Hills, CA, 1989.

19. Carpenter, S.E., and Small, G.W., "Selection of Optimum Training Sets for Use in Pattern Recognition Analysis of Chemical Data," Analytica Chemica Acta Vol. 249, pp 305-321 (1991).

20. Welti, D., Infrared Vapour Spectra, Indices 180-181, Heyden & Son Ltd. with Sadtler Research Laboratories Inc., London, England, 1970.

21. Nakamoto, K., Infrared and Raman Spectra of Inorganic and Coordination Compounds, 3rd ed., pp 151-154, Wiley Interscience Publishers, New York, NY, 1978.

22. Interact Ver. 1.1, Quantitative Spectral Database, Sprouse Scientific Systems, Inc., Paolia, PA, 1991.

23.Boublik, T., Fried, V., and Hala, E., The Vapour Pressures of Pure Substances, p 179 and p 253, Elsevier, Amsterdam, Netherlands, 1984.

24. deHaseth, J.A., and Isenhour, T.L., "Reconstruction of Gas Chromatograms from Interferometric Gas Chromatography/ Infrared Spectrometry Data," Analytical Chemistry Vol. 49(13), pp 1977-1981 (1977).

25. Brissey, G.M., et al., "Comparison of Gas Chromatograph/Fourier Transform Spectrometric Gram-Schmidt Reconstructions from Different Interferometers," Analytical Chemistry Vol. 56(12), pp 2002-2006 (1984).

26. Bjerga, J.M., and Small, G.W., "Reconstruction of Gas Chromatograms from Digitally Filtered Fourier Transform Interferograms," Analytical Chemistry Vol. 61(10), pp 1073-1079 (1989).

27. Savitsky, A., and Golay, M.J.E., "Smoothing and Differentiation of Data by Simplified Least Squares Procedures," Analytical Chemistry Vol. 36(8), pp 1627-1639 (1964).

28. Bialkowski, S.E., "Real-Time Digital Filters: Finite Impulse Response Filters," Analytical Chemistry Vol. 60(5), pp 335A-361A (1988).

29. Duda, R.O., and Hart, P.E., Pattern Classification and Scene Analysis, Wiley Interscience Publishers, New York, NY, 1973.

30. Kaltenbach, T.F., and Small, G.W., "Development and Optimization of Piecewise Linear Discriminants for Automated Detection of Chemical Species," Analytical Chemistry Vol. 63(9), pp 936-944 (1991).

Blank

APPENDIX A

DATA COLLECTION DISK FORMAT

GLOBAL HEADER - 512 BYTES

Byte Position	Bytes Used	Field Description	Data Type
		<<General Information>>	
0	10	Filename (CCC####)	String
10	10	Date (MM/DD/YY)	String
20	10	Start Time (HH:MM:SS)	String
30	10	Stop Time (HH:MM:SS)	String
40	2	Stop Scan Number	Integer
42	10	Operator's Name	String
52	44	Unused	String
		<<Sensor Information>>	
96	20	Sensor Identification	String
116	2	Collection Mode	Integer
118	2	Integer Type	Integer
120	2	Interferogram Pts/Scan	Integer
122	8	Resolution	Double
130	8	Scan Speed	Double
138	8	Mirror Velocity	Double
146	8	Sampling Frequency	Double
154	8	Starting Frequency	Double
162	8	Ending Frequency	Double
170	8	Maximum Wavenumber	Double
178	2	HeNe Zero Crossings/Pt.	Integer
180	16	Unused	String
		<<Weather Information>>	
196	2	Ambient Temperature	Integer
198	8	Barometric Pressure	Double
206	2	Humidity	Integer
208	2	Wind Speed	Integer
210	2	Wind Direction	Integer
212	2	Sensor FOV Direction	Integer
214	2	Precipitation Code	Integer
216	40	Unused	String
		<<Comments>>	
256	64	comment - line #1	String
320	64	comment - line #2	String
384	64	comment - line #3	String
448	64	comment - line #4	String

SUBFILE INTERFEROGRAM HEADER - 64 BYTES

Byte Position	Bytes Used	Field Description	Data Type
0	2	Interferogram number	Integer
2	10	Filename	String
12	10	Time (HH:MM:SS)	String
22	2	Center burst location	Integer
24	2	ADC Gain	Integer
26	2	Number of Averaged Intf.	Integer
28	34	Unused	String
62	2	Error Code	Integer

INTERFEROGRAM POINTS - VARIABLE BYTES

Integer data block consists of consecutive data bytes with data type designated in the global header. The integer data block length is specified by the number of interferogram points per scan (see global header).

APPENDIX B

VAPOR TRAINING SUBSET DESCRIPTION

TRAINING SET DATA - Acetone Vapor Present -

ACTIVE BISTATIC (850)

IR Source	#	Location	Weather	FOV
1.0 V	112	Site 3	Rain	NT
1.5 V	123	Site 2	Fair	T
2.0 V	147	Site 3	Rain	NT
3.0 V	121	Site 3	Rain	NT
4.0 V	110	Site 3	Rain	NT
5.0 V	63	Site 3	Rain	NT
6.0 V	64	Site 3	Rain	NT
8.0 V	48	Site 2	Fair	T
12.0 V	62	Site 2	Fair	T

PASSIVE TERRESTRIAL (89)

IR Source	#	Location	Weather	FOV
Shed	9^{64}	Site 3	Fair	NT
Shed	8	Site 3	Rain	NT
Shed	24	Site 3	Rain	NT
Shed	48	Site 3	Rain	NT

PASSIVE LABORATORY (84)

#	Concentration Vapor	ΔT (°C)
14	×1	29
16	×1	19
15	×1	9
22	×1	-1
17	×1	-11

Note: Superscript on the interferogram count number (#) indicates the number of interferograms averaged per interferogram subfile.

TRAINING SET DATA - MEK Vapor Present -

ACTIVE BISTATIC (1121)

IR Source	#	Location	Weather	FOV
1.0 V	202	Site 3	Cloudy	NT
1.0 V	75	Site 3	Rain	NT
1.5 V	56	Site 4	Fair	T
2.0 V	94	Site 3	Cloudy	NT
2.0 V	199	Site 3	Rain	NT
3.0 V	142	Site 3	Rain	NT
4.0 V	136	Site 3	Rain	NT
5.0 V	71	Site 3	Cloudy	NT
5.0 V	51	Site 3	Rain	NT
6.0 V	71	Site 3	Cloudy	NT
6.0 V	24	Site 3	Rain	NT

PASSIVE TERRESTRIAL (103)

IR Source	#	Location	Weather	FOV
Shed	20	Site 3	Fair	NT
Shed	26	Site 3	Cloudy	NT
Shed	4^{8}	Site 3	Cloudy	NT
Shed	53	Site 3	Rain	NT

PASSIVE LABORATORY (74)

#	Concentration Vapor	ΔT (°C)
15	×1	29
15	×1	19
12	×1	9
16	×1	-1
16	×1	-11

TRAINING SET DATA - SF_6 Gas Present -

ACTIVE BISTATIC (211)

IR Source	#	Location	Weather	FOV
8.0 V	120	Site 1	Rain	T
12.0 V	91	Site 2	Fair	T

PASSIVE TERRESTRIAL (57)

IR Source	#	Location	Weather	FOV
Shed	33	Site 3	Fair	NT
Shed	24[16]	Site 3	Fair	NT

PASSIVE LABORATORY (660)

#	Concentration (cc)	ΔT (°C)
15	0.2	29
16	0.2	19
13	0.2	9
16	0.2	4
23	0.2	1
16	0.2	-11
100	0.04	29
100	0.04	19
61	0.04	9
26	0.04	-1
100	0.04	-11
100	0.08	7
60	0.08	5
14	0.08	4

Blank

APPENDIX C

ACETONE AND SF_6 PLDA SUMMARY

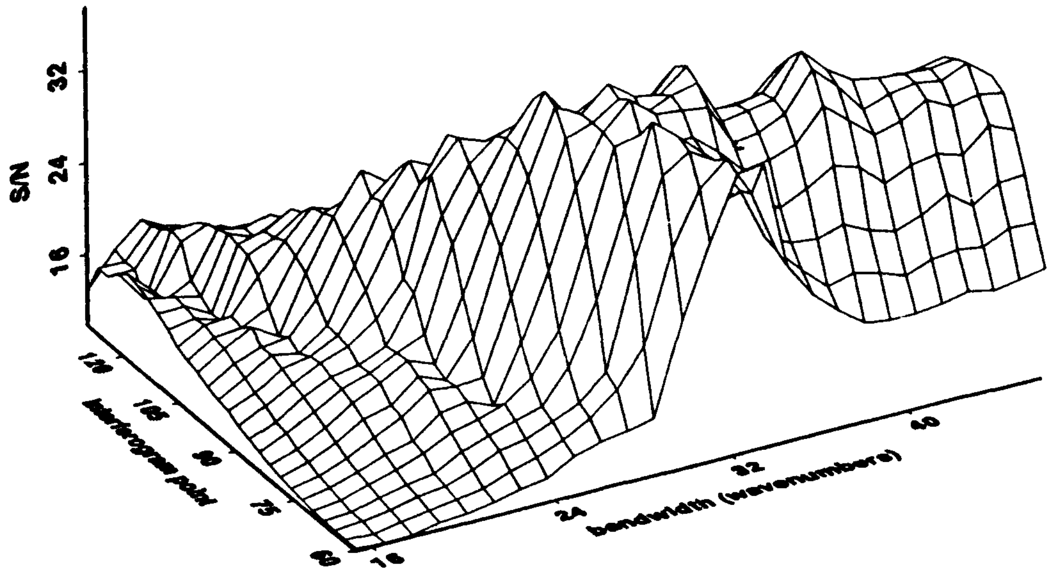

ACETONE FILTER S/N (1187.7 WAVENUMBERS)

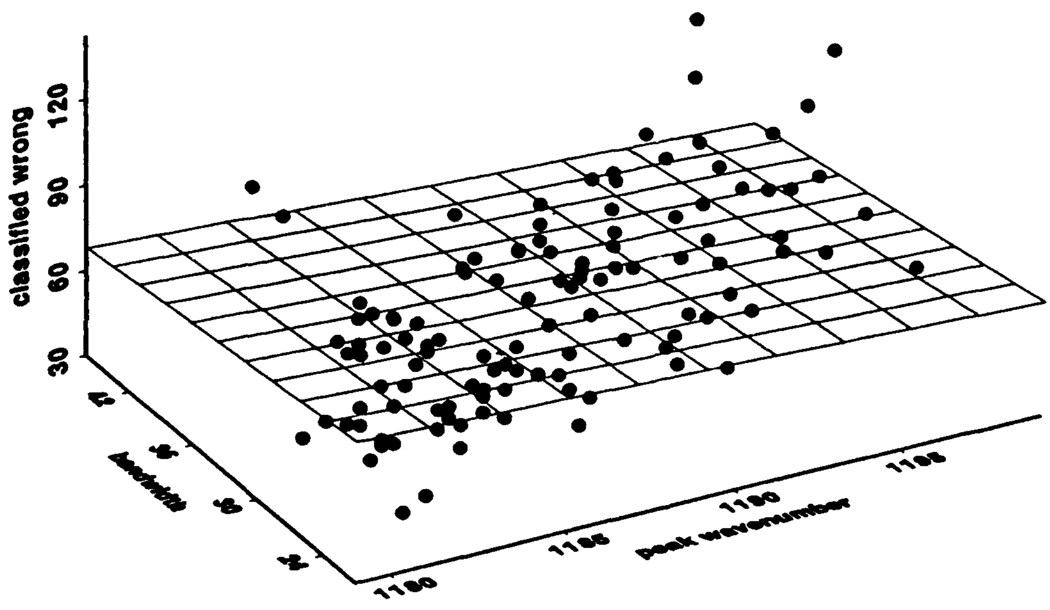

ACETONE PATTERN RESULTS

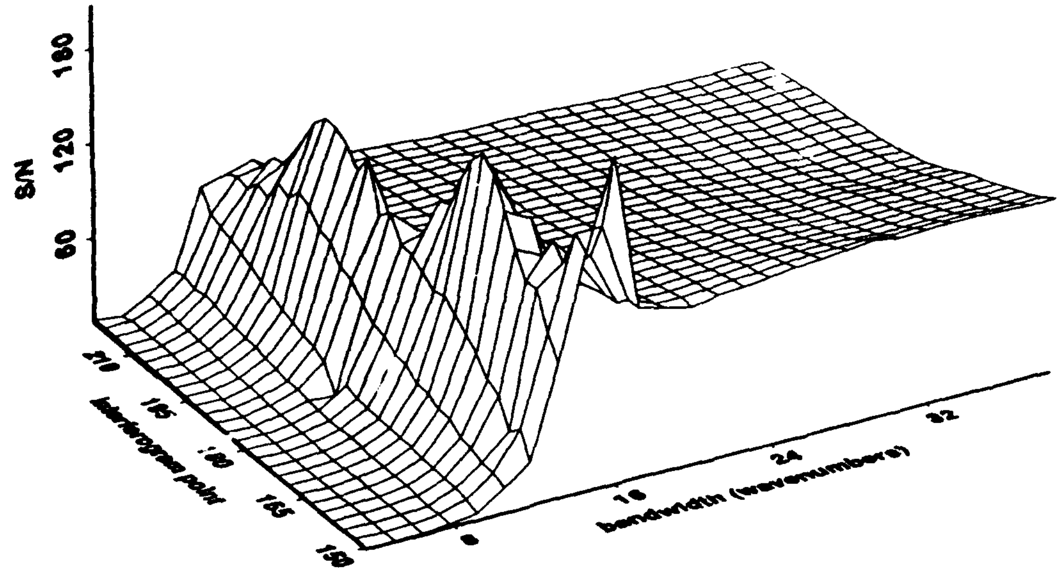

SF6 FILTER (948 WAVENUMBERS)

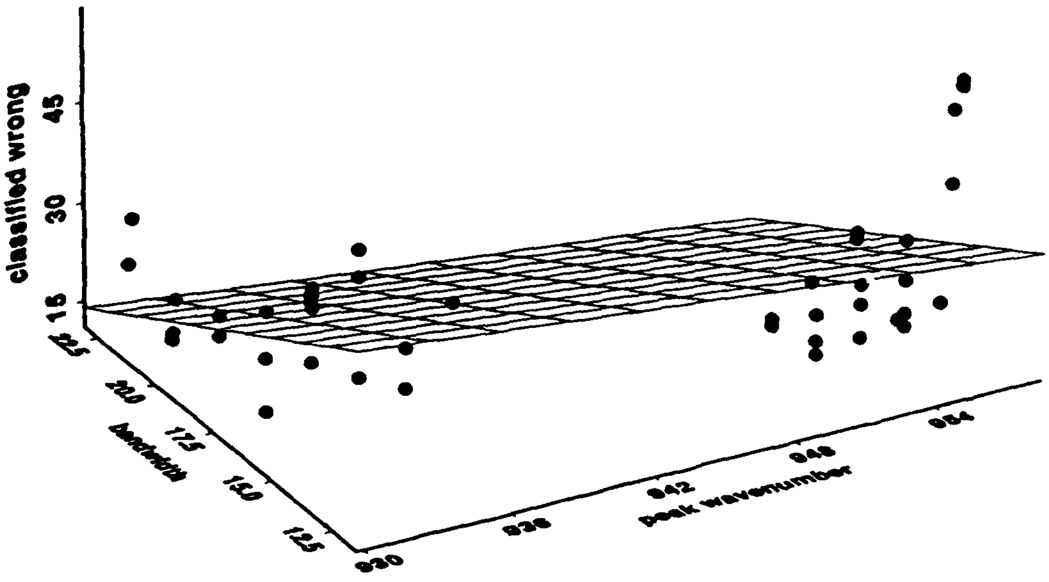

SF6 PATTERN RESULTS

APPENDIX C

APPENDIX D

FIRM FILTER FREQUENCY RESPONSE

1. Select a spectral frequency, ν_j, between 0 and ν_{max}.

   $f_j = 2 \bullet \upsilon \bullet \nu_j$ = interferometer modulation frequency
   υ = interferometer mirror velocity

2. Input the synthetic cosine waveform for the selected spectral frequency.

   $x_{i,j} = \cos(2\pi i(f_j/f_{max}))$
   $x_{i,j}$ = simulated interferogram point at frequency f_j
   i = interferogram point index
   f_j = selected input frequency
   f_{max} = highest frequency response to be calculated

3. Calculate filter response on the logarithmic decibel scale . (dB) using SOS of filtered and unfilter synthetic interferogram segments

   $dB = -20 \bullet \log(Y_j/X_j)$

   $X_j = \sum_{i=1}^{N} (x_{i,j})^2$ input unfiltered segment SOS

   $Y_j = \sum_{i=1}^{N} (y_{i,j})^2$ output filtered segment SOS

4. Oscillatory behavior of frequency response plots due to the discrete number of frequency components used to generate the frequency response and discontinuous interferogram segments used by the FIRM filter.